Building Simulation 2003

Eighth International IBPSA Conference
Eindhoven, Netherlands
August 11-14, 2003

BUILDING MORPHOLOGY, TRANSPARENCE, AND ENERGY PERFORMANCE

Werner Pessenlehner and Ardeshir Mahdavi
Department of Building Physics and Human Ecology
Vienna University of Technology
Vienna, 1040 - Austria

ABSTRACT

Certain energy-related building standards make use of simple numeric indicators to describe a building's geometric compactness. Typically, such indicators make use of the relation between the volume of a built form and its surface area. The indicators are then used along with information on the thermal transmittance of the building enclosure elements to evaluate the degree to which a building design meets the relevant thermal insulation criteria. Using extensive parametric thermal simulations, this paper examines the reliability of such simple compactness indicators for energy-related evaluative assessments given that buildings with the same compactness attribute could differ in enclosure transparence, orientation, and morphology.

1. INTRODUCTION

Prescriptive building energy codes often set minimum requirements concerning thermal properties of building components. To account for the geometry of buildings in a simple manner, some energy-related building standards make use of simple numeric indicators that focus on building's geometric compactness (Heindl and Grilli 1991, Mahdavi et al. 1996, ÖNORM 2002). Typically, such indicators are derived based on the relationship between the volume of a built form and the surface area of its enclosure. The indicators are then used along with information on the thermal transmittance of the building enclosure elements to evaluate the degree to which a building design meets the relevant minimum thermal requirements. However, the usage of geometric compactness for such evaluative purposes could be criticized on multiple grounds. First, compactness does not capture the specific morphology (or the unique three-dimensional formal articulation and massing) of a building's shape, even though it could influence the thermal performance (e.g. via self-shading). Second, compactness does not capture the amount and distribution of the transparent components of the enclosure. Thus, corresponding radiative gains and losses are not accounted for. Third, changing the orientation of a building (e.g., south orientation versus west orientation) does not change its compactness, but may affect thermal performance given changes in insolation and shading conditions.

Given these critical considerations, the present study examines the reliability of geometric compactness indicators for energy-related evaluative assessments based on extensive parametric thermal simulation studies. We explore, via variations of building morphology and transparence (the size and distribution of transparent enclosure components), the limitations of exclusive reference to shapes compactness in thermal performance assessment guidelines and standards. Specifically, we demonstrate the thermally relevant interdependencies between compactness and transparence for a specific climatic context and for a morphologically varied class of residential building shapes.

2. APPROACH

2.1 Overview

The research design for the present study involves the following steps: *i)* A sample of different building shapes is selected, providing morphological variance; *ii)* Different glazing scenarios are generated through variance in glazing area and orientation; *iii)* The resulting set is thermally analyzed via simulation; *iv)* The simulation results (energy load, overheating index) are discussed in the context of the sample's variance in morphology and transparence.

2.2 Shapes

A modular geometry system was derived based on an elementary cube (3.5×3.5×3.5 m). To generate different building shapes, 18 such elements were used (see Figure 1). These elements were aggregated in different ways to create 54 morphological variations. Figure 2 illustrates this set according to their compactness.

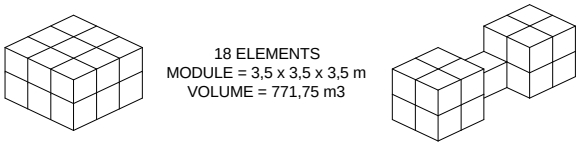

Figure 1 – Generation of shapes based on 18 cubical elements

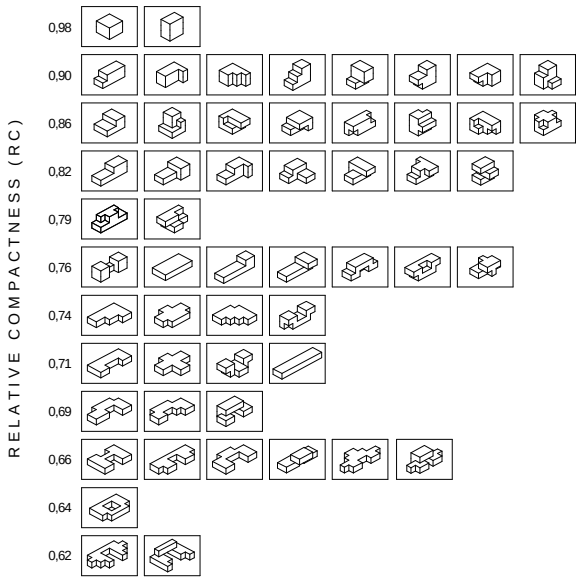

Figure 2 – All generated shapes

To specify compactness, we used the "Relative Compactness" (RC) indicator (Mahdavi u. Gurtekin 2002a). The RC of a shape is derived in that its volume to surface ration is compared to that of the most compact shape with the same volume. For sphere as the reference, it is given by:

$$RC = 4.84 \cdot V^{0.66} \cdot A^{-1} \qquad \text{(eq. 1)}.$$

Since most buildings have orthogonal polyhedronal shapes, we use cube as the reference shape, thus arriving at the following definition of RC:

$$RC = 6 \cdot V^{0.66} \cdot A^{-1} \qquad \text{(eq. 2)}.$$

RC is purely shape-dependent, in contrast to conventional compactness indicators such as characteristic length (l_c) which depend on the shape's size (i.e., absolute value of the volume):

$$l_c = V \cdot A^{-1} \qquad \text{(eq. 3)}.$$

Since our main morphological sample involves shapes of equal volumina, RC and l_c could be used interchangeably to characterize shape compactness. We prefer to use RC, though, as previous studies have indicated that it better describes the subjective (perception-based) categorization of shape compactness by designers (Mahdavi u. Gurtekin 2002a). Moreover, l_c can be easily derived from RC if necessary:

$$l_c = RC \cdot V^{0.66} \cdot 6^{-1} \qquad \text{(eq. 4)}.$$

From the sample shown in Figure 2 a subset of 12 shapes with distinct RC values was selected for the simulations (see Figure 3).

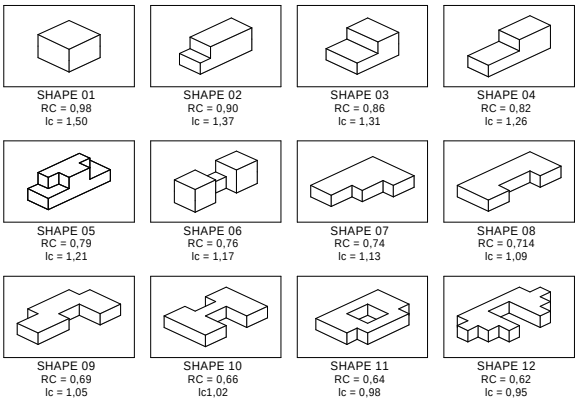

Figure 3 – The 12 shapes selected for simulation

To achieve variation in enclosure transparence, the amount of glazing and its distribution across the enclosure walls was changed. Concerning glazing area, three levels were considered, namely 10%, 25%, and 40% glazing, expressed as fraction of the gross floor area (Figure 4). Subsequently, the glazing area was distributed across the enclosure in five different ways, as per Table 1. In addition, the shapes were rotated four times in intervals of 90 degrees (Figure 5). Given 12 shapes, 3 glazing area options, 5 glazing distribution options, and 4 orientations, a total of 720 variations were thus generated for simulations.

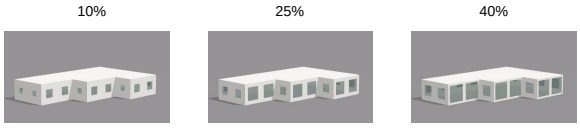

Figure 4 – Illustration of the variation of the glazing percentage (fraction of gross floor area)

Table 1 – Variations of transparence

Variation	Percentage of glazing facing: North	East	South	West
Uniform	25	25	25	25
North	55	15	15	15
East	15	55	15	15
South	15	15	55	15
West	15	15	15	55

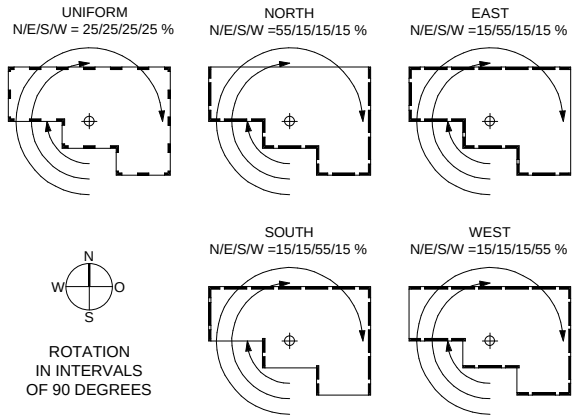

Figure 5 – Glazing area distribution

2.3 Invariant assumptions

A number of parameters were kept constant throughout the simulations, namely location (Vienna, Austria), building use (residential), building volume (772 m^3), building construction, internal heat gains, and air change rates. The assumptions regarding thermal transmittance and surface density values of the primary building components of the model are summarized in Table 2. Lighting and equipment loads, as well as the number of people were assumed to be dependent on the time of day, amounting to an average value of approximately 5 $W.m^{-2}$. Air change rates were varied from 0.5 to 2 h^{-1} according to the time of the year.

Table 2 – Building components properties

Building component	Surface density [$kg \cdot m^{-2}$]	U [$W \cdot m^{-2} \cdot K^{-1}$]
Floor	850	0.33
External wall	310	0.21
Roof	860	0.16
External floor	620	0.20
Window	20	1.10

2.4 Simulations

Simulations were performed using the application NODEM (Mahdavi u. Mathew 1995). The simulation results were expressed in terms of two performance indicators, namely annual heating load (in $kWh \cdot m^{-2} \cdot a^{-1}$) and overheating index (in $Kh \cdot a^{-1}$). The latter was defined as the sum of hourly temperature differences between the room temperature and an overheating reference temperature (27^o during day and 25^o in the night). This reference temperature is currently applied in Austria for residential buildings (ÖNORM 1999).

3. RESULTS

Figure 6 shows (for all simulated instances) the relationship between heating load and RC. The respective correlation is fairly high (R^2=0.88). If the results are sorted according the glazing percentage (see Figure 7), even higher correlations emerge (R^2=0.95 for 10% glazing, 0.94 for 25%, and 0.90 for 40%). Larger glazing areas result in slightly lower heating loads (increased solar gains apparently outweigh increased transmission losses). A further distinction of the results in terms of the distribution of glazing (see Figure 8 for 25% glazing area option) reveals still higher correlations (0.97 for uniform and north, 0.95 for south, 0.96 for west and east). These results confirm the expectation that dominantly south-oriented glazing results in the lowest heating load, whereas dominantly north-oriented glazing results in the highest heating load.

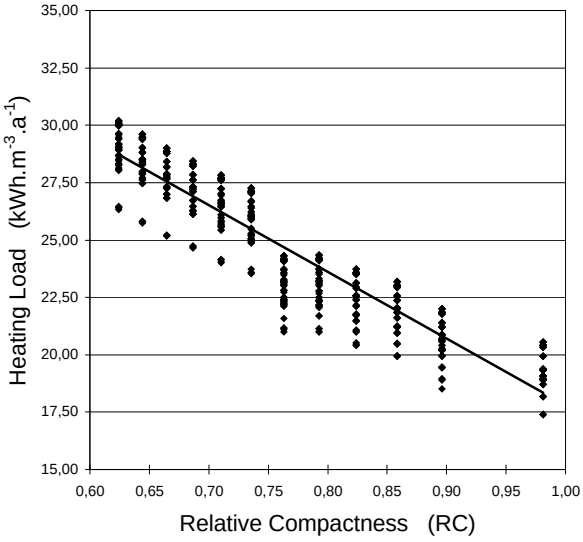

Figure 6 – Simulated heating loads as a function of RC (all instances)

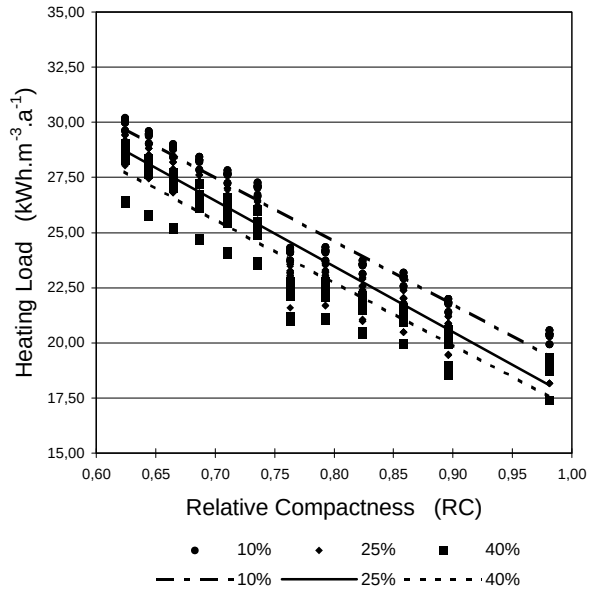

Figure 7 – Simulated heating loads as a function of RC and glazing percentage (10%, 25%, and 40%)

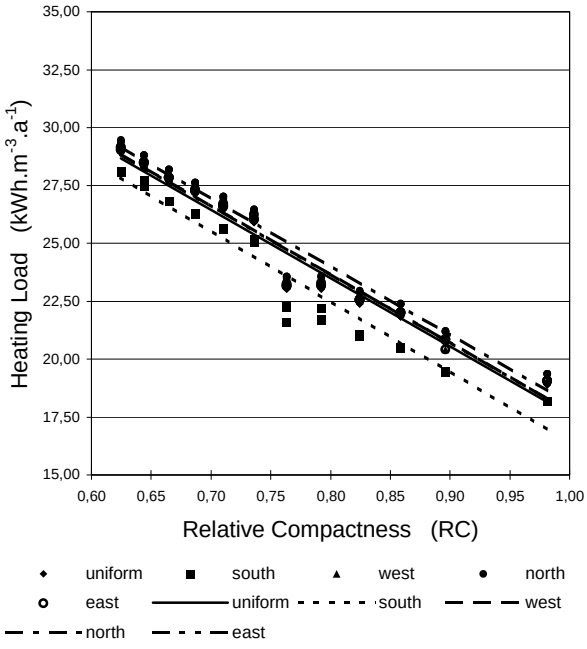

Figure 8 – Simulated heating loads as a function of RC and glazing distribution options (for 25% glazing option)

While from the simulation results a significant association between heating load and RC can be inferred, the association between overheating and RC is relatively week. Since simulations for 10% and 25% glazing areas did not result in noteworthy overheating occurrences, only the results for 40% glazing are given in Figure 9 (R^2=0.59). If these results are grouped based on the orientation of glazing (see Figure 10), higher correlations emerge (0.93 for uniform, 0.88 for south, 0.87 for west, 0.84 for north, and 0.86 for east). The higher occurrence of overheating for the south exposure (as compared to east and west) is mainly due to the longer duration of the south façade's solar exposure.

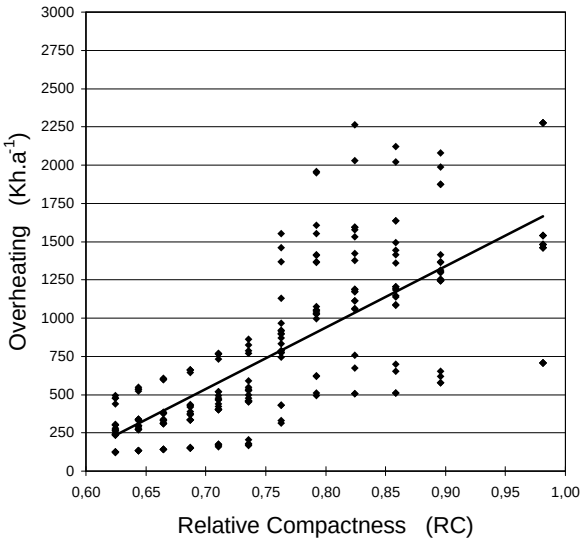

Figure 9 – Simulated overheating as a function of RC (all instances with 40% glazing)

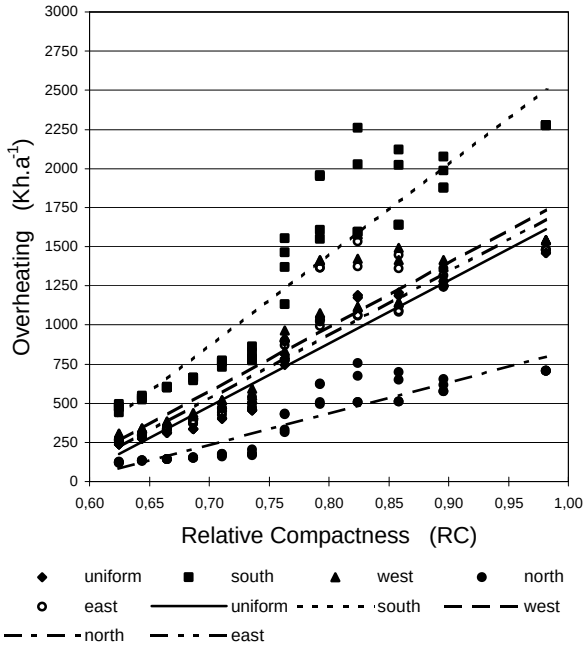

Figure 10 – Simulated overheating as a function of RC and glazing distribution options (all instances with 40% glazing)

4. DISCUSSION

A solid association between RC and heating load can be inferred from the sample of shapes considered in this study. More compact shapes result indeed in somewhat smaller heating loads. RC seems to capture geometry well, despite its negligence of the morphological variance of the sample. Distinctions regarding transparence (amount and orientation of glazing) allow to further refine this association, but do not change its general trend. Moreover, given low U-value glazing systems, increased glazing area can – contrary to the conventional wisdom – reduce heating load, whereby increased transmission losses through the enclosure are more than compensated by increased solar heat gains.

While overheating tendency increases with increasing RC, the association is much weaker in this case. Overheating is significantly affected by the amount of the glazing (in the present study, it did not occur for glazing areas under 30%). Moreover, the orientation of glazing has a clear influence on the resulting overheating. As expected, a south-dominant glazing orientation results in significantly higher overheating than the north-dominated glazing orientation. The deviation of the individual results from the general trend are generally large, implying that RC does not sufficiently capture those morphological properties of the design (such as self-shading) that could be relevant to the occurrence of overheating.

To further contrast the performance of RC in the case of heating load to its performance in the case of overheating, we consider the errors that occur, when heating load and overheating predictions are made based on regression equations. Figure 11 illustrates the relative deviation of individual simulation results for heating load (for 40% glazing area) from the corresponding predictions made based on linear regression (cp. Figure 7). Deviations lie in this case between -10% and +10%. Figure 12 illustrates the relative deviation of individual simulation results for overheating from the corresponding predictions made based on linear regression (cp. Figure 9). Deviations are in this case much larger and lie between -75% and +125%.

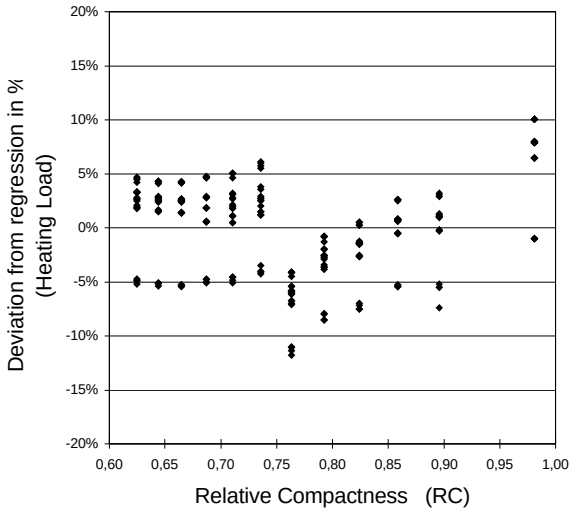

Figure 11 – Deviation of simulated heating loads from regression-based predictions (for 40% glazing option)

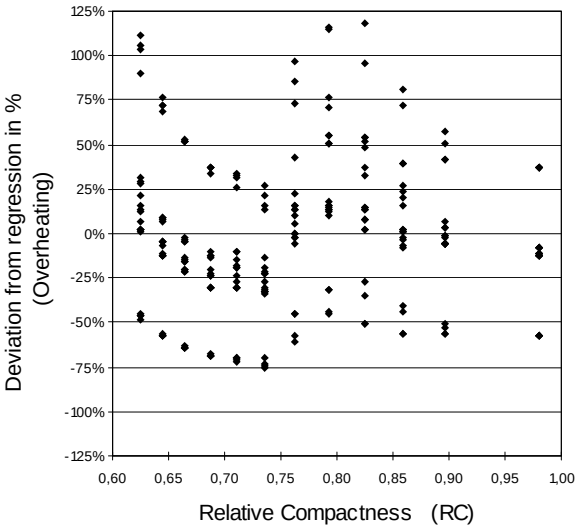

Figure 12 – Deviation of simulated overheating results from regression-based predictions (for 40% glazing option)

5. ADDITIONAL EXPLORATIONS

5.1 Different shapes

In the previous discussion, we dealt with a sample of 12 shapes with distinct RC values. To explore the potential effect of morphological variance not accounted for by RC, we selected (from figure 2) five morphologically distinct shapes with the same RC value of 0.86 (Figure 13) for further simulation studies. Heating loads and overheating were computed for these shapes, whereby the same glazing options and distributions were considered as in the previous study (cp. Sections 2.2, 2.3, 2.4). Figure 14 illustrates the deviation of the simulated heating loads for these five shapes from predictions based on the regression equation of the original sample (cp. Figure 6). Figure 15 illustrates the deviations of the simulated overheating values for the five shapes from predictions based on the regression equation of the original sample (cp. Figure 9). A comparison of the error ranges of the sample of these five shapes with the error ranges of the original 12 shapes sample is presented in Table 3. The deviations resulting from shape variance are in the case of heating load in the same order of magnitude as the deviations of the original sample, and in the case of overheating somewhat larger than the deviations of the original sample. These results imply that regression-based heating load predictions can reasonably rely on RC as geometry indicator, despite morphological variance. However, such predictions are not reliable in the case of overheating and are further compromised due to morphological attributes not captured by RC.

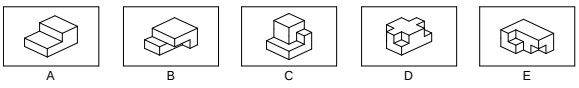

Figure 13 – Sample of five distinct shapes with the same RC value (RC = 0.86)

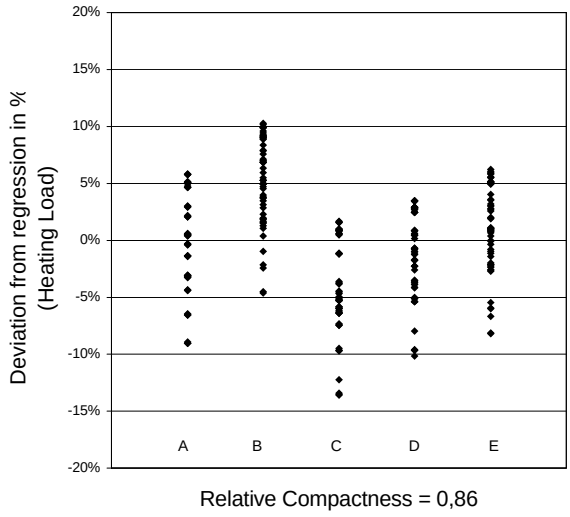

Figure 14 – Deviation of simulated heating loads (for the sample of five shapes with identical RC values) from regression-based predictions of the original sample (cp. Figure 6)

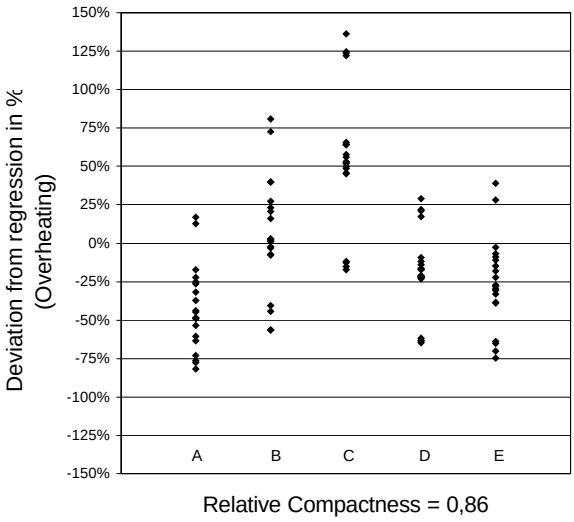

Figure 15 – Deviation of simulated overheating results (for the sample of five shapes with identical RC values) from regression-based predictions of the original sample (cp. Figure 9)

Table 3 – Comparison of regression-based prediction errors: five shapes sample versus original sample

	Deviation range for:	
	5 shapes sample	Original sample
Heating load	-15 to +10 %	-15 to +12%
Overheating	-80 to +130%	-75 to +125%

5.2 Different volumina

The original study dealt with shapes of the same volume (772 m^3). To explore the implications of changes in volumina, a new sample was generated based on a subset of the shapes in the original sample shown in Figure 3. We selected five shapes with distinct RC values. We further assumed three possible volumina for each shape (the original volume of 772 m^3, as well as 2680 m^3 and 6174 m^3). The simulations were performed for the 25% glazing option only. Since RC is not volume-dependent, Figure 16 illustrates the simulated heating loads as a function of both RC and volume. Figure 17 illustrates the same results as Figure 16 but instead of RC, it uses the volume-dependent l_c as the compactness indicator. These results imply that simulated heating loads (HL) can be reproduced via regression-based functions fairly well, even when dealing with shapes of different volumina. Accordingly, the association implied in figure 17 can be represented via the following (equivalent) equations:

$$HL = 27 \cdot l_c^{-0.75} \qquad \text{(eq. 5)}$$

$$HL = 105 \cdot RC^{-0.75} \cdot V^{-0.25} \qquad \text{(eq. 6)}$$

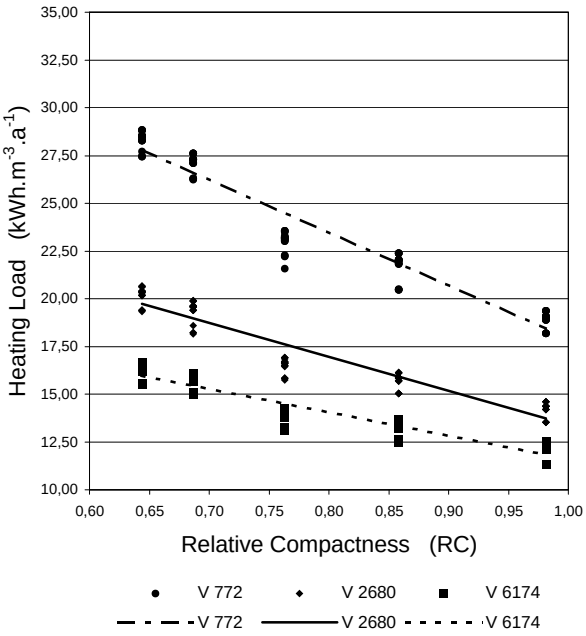

Figure 16 – Heating load of sample C as a function of RC (for three volume ranges and 25% glazing option)

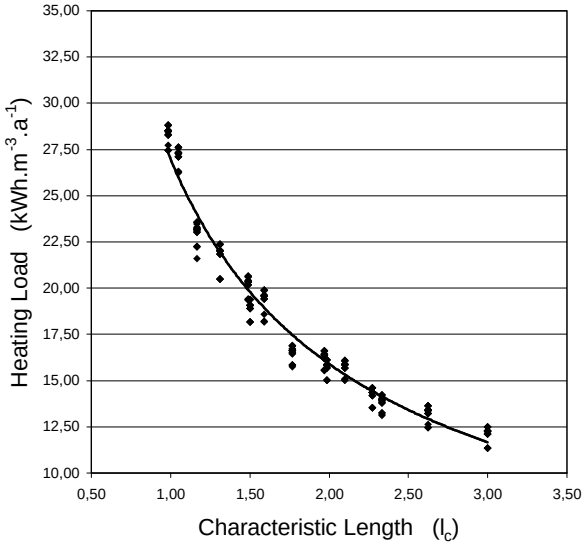

Figure 17 – Heating load of sample C as a function of l_c (for the 25% glazing option)

6. CONCLUSION

Given the context and boundary conditions of the present study, the reliability of simple indicators of building geometry such as compactness indicators RC and l_c must be seen differentially. The association between the values of such indicators and simulated heating loads of buildings with various shapes, orientation, glazing percentage, and glazing distribution was found to be significant. Accordingly, the use of such indicators in energy standards (for heating load prediction and evaluation purposes) may be justified. However, these indicators do not appear to capture the geometry of a building to the extent necessary for the predictive assessment of the overheating risk.

Beyond their potential for relevant codes and standards, reliable and intuitive numeric indicators of geometry could be adopted as a design dimension of the "design-performance space", which denotes a virtual space defined by multiple design and performance dimensions (Mahdavi u. Gurtekin 2002b). In this space, each design dimension accommodates the range of possible values of a discretized design variable. Design variables can capture various geometric (volume, shape, compactness) and semantic (thermal transmittance of the building enclosure, thermal mass, internal loads) features of design. Likewise, each performance dimension accommodates the range of the values of a specific performance indicator (e.g., energy use, reverberation time in rooms, illuminance levels on working planes). The design-performance space can provide an effective context for the assessment and comparative evaluation of the performance of alternative building designs in the early stages of the design process.

7. REFERENCES

Heindl, W., Grilli, P.V. 1991. On Establishing Standards for the Overall Heat Transfer Coefficient of Buildings, *CIB-W67-Workshop 1991*, Vienna.

Mahdavi, A., Gurtekin, B. 2002a. Shapes, Numbers, and Perception: Aspects and Dimensions of the Design Performance Space, *Proceedings of the 6th International Conference: Design and Decision Support Systems in Architecture*, The Netherlands, ISBN 90-6814-141-4. pp 291-300.

Mahdavi, A., Gurtekin, B. 2002b. Adventures in the design-performance space, *Proceedings of the 16th European Meeting on Cybernetics and System Research*. Vienna, Austria. Volume 1, pp. 269-274.

Mahdavi, A., Mathew, P. 1995. Synchronous generation of homologous representations in an active, multi-aspect design environment, *Proceedings. of IBPSA Conference*. 31(5), pp 522-528.

Mahdavi, A., Brahme, R., Mathew, P. 1996. The "LEK"-Concept and its Applicability for the Energy Analysis of Comercial Buildings, *Building and Environment*, 31(5). pp 409-415.

ÖNORM 2002. ÖNORM B 8110-1: Wärmeschutz im Hochbau – Anforderungen an den Wärmeschutz und Nachweisverfahren, *Österreichisches Normungs-institut*, Wien, 29. Januar 2002.

ÖNORM 1999. ÖNORM B 8110-3: Wärmeschutz im Hochbau – Wärmespeicherung und Sonneneinflüsse, *Österreichisches Normungsinstitut*, Wien, 1. Dezember 1999.